Pure appl. geophys. 163 (2006) 1787–1801
0033–4553/06/091787–15
DOI 10.1007/s00024-006-0097-z

Pure and Applied Geophysics

Numerical and Experimental Study on Progressive Failure of Marble

Robina H. C. Wong,[1] M. R. Jiao,[1,2] and K. T. Chau[1]

Abstract—This study presents a framework for numerical simulations based upon micromechanical parameters in modeling progressive failures of heterogeneous rock specimens under compression. In our numerical simulations, a Weibull distribution of the strength and elastic properties of the finite elements is assumed, and the associated Weibull parameters are estimated in terms of microstructural properties, such as crack size distribution and grain size, through microscopic observations of microcracks. The main uncertainty in this procedure lies on the fact that various ways can be used to formulate a "microcrack size distribution" in relating to the Weibull parameters. As one possible choice, the present study uses the number of counted cracks per unit scanned volume per grain size to formulate the crack distributions. Finally, as a tool, the Rock Failure Process Analysis code ($RFPA^{2D}$) is adopted for simulating the progressive failure and microseismicity of heterogeneous rocks by using an elastic-damage finite-element approach. To verify our framework, compression tests on marble specimens are conducted, and the measured acoustic emissions (AE) are compared with those predicted by the numerical simulations. The mode of failure, compressive strength and AE pattern of our simulations basically agree with experimental observations.

Key words: Heterogeneous rocks, Weibull parameters, crack distributions, acoustic emissions, microseismicity, numerical simulation.

Introduction

Brittle fracture has been intensively investigated in the areas of rock mechanics and rock engineering. A number of studies have been done to investigate the fracturing process of rock using an optical microscope (Mowar *et al.*, 1996; Homand *et al.*, 2000), or scanning electron microscope (SEM) (Wu *et al.*, 2000; Heidelbach *et al.*, 2000). These kinds of studies can provide the knowledge on the progressive failure of rock. However, the microscopic observations are limited to the surface of the specimen. To capture the failure process within a rock specimen and the induced microseismicities during failure process, acoustic emission (AE) detection (Young and Collins, 2001; Dobson *et al.*, 2004) or an X-ray computerized tomography (CT) scanning system have been used, (Kawakata *et al.*, 1999;

[1] Civil and Structural Engineering Department, The Hong Kong Polytechnic University, Hung Hom, Hong Kong, China. E-mail: cerwong@polyu.edu.hk; cektchau@polyu.edu.hk
[2] Liaoning Seismological Bureau, Shenyang, 110031, China. E-mail: mrjiao@yahoo.com

FENG *et al.*, 2004). Incorporation of AE or CT measurements with surface observations leads to a better understanding of the progressive failure of rocks under compression.

Recently, a number of numerical models were developed to capture the growth, interaction and coalescence of the pre-existing microcracks. Successful numerical models have been proposed to simulate rock failure study by considering the heterogeneity of materials using the Weibull distribution (TANG *et al.*, 1998; FANG and HARRISON, 2002; YUAN and HARRISON, 2004). In the Weibull distribution model for heterogeneity, both elastic moduli and strength parameters can be characterized by a set of Weibull parameters as (m and σ_o), where m and σ_o are the heterogeneous index and the average mechanical property (either modulus or strength) at the element level. Physically, a smaller m implies a more heterogeneous distribution of properties, and vice versa. One main limitation of such an approach is that the values of both m and σ_o are estimated purely by trial and error procedure in previous studies (LIN *et al.*, 2000; LIU *et al.*, 2004; TANG *et al.*, 2001) since there has been no theoretical basis for estimating these Weibull parameters. Recently, WONG *et al.* (2004, 2006) and JIAO *et al.* (2004) proposed a theoretical framework to determine m and σ_o quantitatively in terms of these microstructural attributes, such as grain size and microcrack statistics. Preliminary trials have been conducted by WONG *et al.* (2004) and JIAO *et al.* (2004) in relating the Weibull parameters to Yuen Long marbles found in Hong Kong. However, we subsequently realize that there are various ways of interpreting the microcrack statistics distribution in getting m and σ_o (WONG *et al.*, 2006).

The purpose of this paper is to propose another way of interpreting the Weibull parameters from the microcrack data. In particular, the main difference of the present microcrack data analysis from the previous one (WONG *et al.,* 2004, 2006; JIAO *et al.*, 2004) lies on the fact that the crack distribution is expressed in terms of crack number per total scanned area per unit thickness per grain size, whereas in our preliminary analysis crack number per unit volume and per unit length are assumed (see Fig. 1 in JIAO *et al.*, 2004). The rationale for the present change is that the number of crack count should be sensitive to the scanned volume as well as the grain size (note that, as to be shown later, the crack size distribution has to be in the unit of crack number per length to the power four).

For the present study, a particular type of marble from mainland China was used as an example. The average gain size of this Chinese marble is 0.52 mm, compared to 0.36 mm for Yuen Long marble used in our earlier study. For our laboratory study, acoustic emissions (AE) during the cracking process are monitored and recorded. A commercial code called "Rock Failure Process Analysis" ($RFPA^{2D}$) (TANG *et al.*, 1998) is used for numerical simulations in the present study, however we expect that similar results will be produced even if another similar numerical code is used. The main issue here is how to interpret the Weibull parameters from raw microcrack data, instead of the use of a particular finite element method (FEM). The $RFPA^{2D}$ is

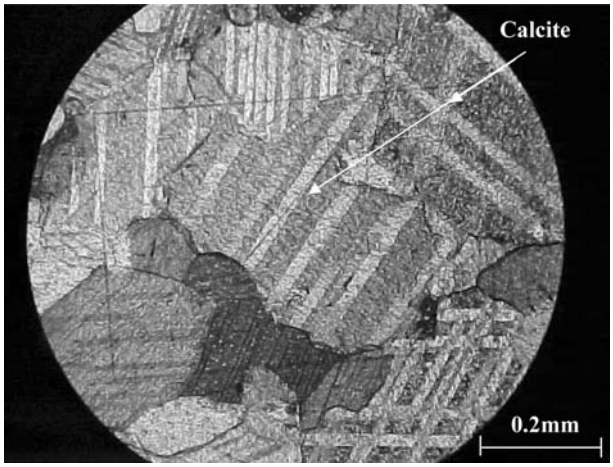

Figure 1
Marble specimen under polarizing microscope.

selected here because microseismicity (or acoustic emissions) are generated during the simulations, and they can be used directly to compare with our experiments on this Chinese marble.

Micromechanical-based Weibull Parameters

The determination of the Weibull parameters (m and σ_o) in terms of the micromechanical properties was first derived by Professor Teng-fong Wong of the State University of New York as presented in reference (WONG *et al.*, 2004, 2006). Thus, in the present section, only the essence is summarized.

Because of the grain-scale heterogeneity, the failure strength of polycrystalline rock can vary for the same type and size of rock specimen. To analyze the statistical variation of the bulk failure strength in heterogeneity material, WEIBULL (1951) adopted the statistics of the cumulative probability function (WEIBULL, 1951) to characterize the failure strength σ:

$$P(\sigma) = 1 - \exp\left[-\left(\frac{\sigma}{\sigma_o}\right)^m\right] \tag{1}$$

in terms of the Weibull parameters m and σ_o. Physically, this distribution given in (1) reflects the inevitable heterogeneity of solids (i.e., no solid is absolutely homogeneous). For rocks, the heterogeneity is caused by the probabilistic aspects of the microstructures, and particularly of the microcrack size distribution. It is well known that a brittle solid containing a longer crack is easier to load to failure than a solid containing a shorter crack LAWN (1993). Thus the length statistics of the long cracks can be described by an extreme value distribution of the Cauchy type: $g(a) = [q^*/a]^Z$,

where a is half crack length, z is a microcrack size distribution index or called the fractal index, q^* is an external parameter depending on the types of rocks. To interpret this distribution, we assume that the cumulative probability function for the cracks in the elemental volume V_0 to have size longer than a_1 is given by $V_o \int_{a_1}^{\infty} g(a)\, da$ (ARGON, 1974; MCCLINTOCK and ARGON, 1966). For a solid of volume V that contains many elemental volumes V_0, if it is assumed that the failure in each elemental volume represents an independent event, then the cumulative probability for failure in V to arise from cracks with lengths longer than a_1 is as follows (ARGON, 1974; MCCLINTOCK and ARGON, 1966):

$$\begin{aligned} P &= 1 - \exp\left[V \int_{a_1}^{\infty} g(a) da\right] = 1 - \exp\left[-\frac{(q*)^z}{(z-1)} \frac{V}{(a_1)^{z-1}}\right] \\ &= 1 - \exp\left[-\frac{V}{V_o}\left(\frac{a'}{a_1}\right)^{z-1}\right] \end{aligned} \tag{2}$$

where the parameter a' is defined by the following relation

$$(a')^{z-1}/V_o = (q*)^z/(z-1). \tag{3}$$

Again, V_o is the representative element volume. Considering that the crack size distribution can be related to fracture probability by applying fracture mechanics concepts, the probability that the stress intensity factor $K = Y\sigma\sqrt{a}$ ($Y = \sqrt{\pi}$ if we assume the crack is isolated and under uniform far-field stress) is equal to the critical value K_{IC} at stress less than σ is given by:

$$P(\sigma) = 1 - \exp\left[-\frac{V}{V_o}\left(\frac{\sqrt{a'}\,\sigma\, Y}{K_{Ic}}\right)^{2z-2}\right]. \tag{4}$$

By equating equations (1) and (4), the Weibull parameter m can be related to the crack size distribution as $m = 2z - 2$. The Weibull parameter σ_o that represents the mean strength for the volume V of an element in the finite-element grid can be evaluated as

$$\sigma_o = (V/V_o)^{-1/m} K_{Ic}/(\sqrt{a'}\, Y). \tag{5}$$

Therefore, the Weibull parameters (m, σ_o) can now be determined from micromechanical parameters. The actual evaluation of these parameters from microcrack data will be discussed next.

Experimental Studies

Physical Properties Testing of Marble and AE Measurement

The rock specimens used in this study are white marble purchased from mainland China. The mechanical and physical properties of this Chinese marble that have been

tested include uniaxial compressive strength σ_c, tensile strength σ_t, Young's modulus E, Poission's ratio υ and density ρ. These tests were conducted in accordance with the testing standards of ASTM (1995a–d). Fractures toughness K_{IC} is determined in accordance with the standard testing method of ISRM (International Society for Rock Mechanics) using Chervon Bend (V-notch) specimen (ISRM, 1988). The results of these tests are listed in Table 1.

Microcrack Study for Marble

The micromechanical basis of Weibull parameters (m, σ_0) [$m = 2z - 2$ and $\sigma_o = (V/V_o)^{-1/m} K_{IC}/\sqrt{a'}Y$)] is determined by using the microcrack statistics. To investigate the statistics of microcracking in marbles, an optical microscope with fine resolutions has been used for microcrack counting. The magnification of the optical microscope used in this study is 100x. A thin section of rock specimen with a size of 45 mm × 25 mm × 3 mm is prepared according to the standard method of ISRM (BROWN, 1981). The final thickness of the thin section is grounded to 0.03 mm. Ten areas (each area of 7.8 mm^2) are randomly selected on the thin section for measuring the distribution of crack length. Typically each scanned area under the optical microscopy covers a minimum of six grains (Fig. 1) and therefore both intragranular and transgranular cracks can be observed. The crack statistics is done based on a sample of more than 60 grains. The Chinese marble specimen consists of uniformly distributed recrystallized calcites. The average grain sizes (D) and crack length $2c$ for the marble are listed in Table 2. Most of the pre-existing microcracks are intragranular, but there are also some transgranular cracks.

The sample measurement is covered over a total area A = 10 × 7.8 mm^2, and the half crack length data are mainly grouped into a length interval of 0.025 mm. The microcrack data are fitted to a power law to determine the parameters z and $(q^*)^z$. It

Table 1

Physical properties of marble

σ_c (MPa)	σ_t (MPa)	E (GPa)	υ	K_{IC} (MPa $m^{1/2}$)	ρ (kg/m^3)
65.74	5.06	47.74	0.289	0.865	2713

Table 2

Microcrack statistics and micromechanical parameters

Grain size D (mm)	Average crack length $2C$ (mm)	z [Fig. 1b]	m ($m = 2z-2$)	$(q^*)^z$ (mm^{z-4}) [Fig. 1b]	V_o ($V_o = \pi \times D^2/4 \times t$) ($mm^3$)	Characteristic crack length a' (3) (mm)	K_{Ic} of calcite (POTYONDY *et al.*, 1996) (MPa $m^{1/2}$)	σ_0 (5) (MPa)
0.52	0.123	1.878	1.76	0.0017	0.229	0.00015	0.2	290.2

is noted from eq. (3) $[(a')^{z-1}/V_o = (q*)^z/(z-1)]$ that the unit for g(a) [$g(a) = (q^*/a)^z$] is mm^{-4}. Therefore, it can be inferred that the values of $(q^*)^z$ is in unit of $mm^{(z-4)}$. As mentioned in the Introduction, there is a flexibility of choosing the dimension for yielding the resulting unit of mm^{-4}. In an attempt to improve our earlier studies, the crack length distribution g(a) is evaluated as the number of microcracks (N) observed from a length interval over the total volume (measured area times uniform thickness $A \times t$; A $= 10 \times 7.8$ mm^2; $t = 1$) and the average grain size D [i.e., $g(a) = N(a)/(10 \times 7.8 \times 1 \times \mathrm{D})$]. This choice is based on the rationale that the number of counted cracks should be scaled by the actual scanned area, that the microcracks are mainly two-dimensional in the thin section, and that the number of microcracks is controlled by grain size. However, we should emphasize that the current combination is only one possible choice in setting up $g(a)$, and it is by no means unique. The curve fitting and Weibull parameters inferred from microcrack statistics is shown in Figure 2 and listed in Table 2.

The z parameter is determined by the power-law function of $g(a) = 0.0017\mathrm{x}^{-1.8776}$ (see Fig. 2). Therefore, z is equal to 1.8776 and thus $(q^*)^z = 0.0017$ mm^{z-4}, respectively. Consequently, m ($m = 2z - 2$) value is then calculated as 1.76. The characteristic crack length a' is calculated by (3) as $(a')^{z-1}/V_o = (q^*)^z/(z-1)$. In a two-dimensional model, the ratio elemental volume is equal to $\mathrm{V_o} = \pi \times D^2/4 \times \mathrm{t}$. The characteristic crack length a' is calculated of 0.00015 mm. The parameter of σ_o is determined by $\sigma_o = (V/V_o)^{-1/m} K_{IC}/\sqrt{a'}\mathrm{Y}$. The parameter Y is a geometric constant and is chosen as $\sqrt{\pi}$ by neglecting the crack-crack interactions. Since the average crack length is smaller than the average grain size of calcite, fracture toughness K_{IC} of calcite mineral of 0.2 MPa $m^{1/2}$ is selected (ATKINSON, 1987). It is further assumed that the size of the finite-element grid is the same as the size of the grain ($V/V_o = 1$).

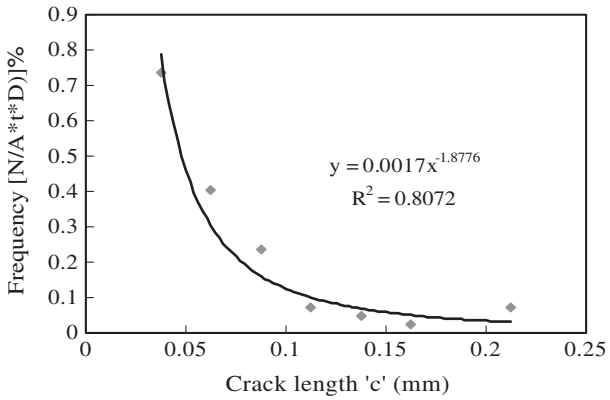

Figure 2
Frequency of crack vs. half size of crack length. The frequency of crack is defined as a number of microcracks (N) over total measured volume ($A \times t = 10 \times 7.8 \times 1$) and the average grain size (D).

With the known parameters, the average elemental strength σ_0 is calculated of 290.2 MPa from (5).

AE Measurement

The uniaxial compression test was conducted using a servo-control MTS compression machine with the loading rate of 0.0005 mm/s at the Rock Mechanics Laboratory of Hong Kong University. A rectangular specimen (50 mm × 25 mm × 110 mm) was compressed to failure with the associated acoustic emissions recorded by four sensors (5 mm diameter) with a frequency of 480 kHz. These sensors were mounted onto the rock surface by epoxy resin. The detected AE wave signals were pre-amplified and then fed into transient recorders at a sampling rate of 1 MHz. The noise threshold is set at 40 dB. The AE signals are recorded by using the MISTRAS-2001 AE recording software and the data are transferred to a computer. Figure 3(a) shows the stress-strain curve of the tested marble versus the AE events plotted on Fig. 3(b). The uniaxial compressive strength of the Chinese marble is 58.51 MPa (Fig. 3(a)) with a mixed shear-tensile mode of final failure, as shown in Figure 3(c). The maximum number of AE events at failure is 534.

A total of 1289 AE events were recorded by the sensors, but most of the released energy was released during a few events near the peak strength. According to MOGI (1962), the seismic pattern of the Chinese marble is a "main-shock type". In particular, MOGI (1962) studied fracture phenomena for various brittle materials with different degrees of heterogeneity. He found that the main-shock type seismic pattern occurred in relatively homogeneous rocks. Our finding agrees with his general conclusion. To compare our experimental finding with our micromechanical-based interpretation of Weibull parameters of heterogeneity, a finite-element code RFPA has been used to simulate the uniaxial compressive strength, the failure patterns and the associated AE events. The results of these numerical simulations will be summarized in the next section.

Numerical Simulation

RFPA^{2D} Model

The code RFPA^{2D} (Rock Failure Process Analysis) (TANG *et al.*, 1998) is based on an elastic finite-element model incorporated with a damage criterion to judge the failure of individual elements, and it has been successfully used to simulate the deformation and failure process of brittle solids (LIN *et al.*, 2000; LIU *et al.*, 2004; TANG *et al.*, 2001). A brief outline of RFPA^{2D} is presented here.

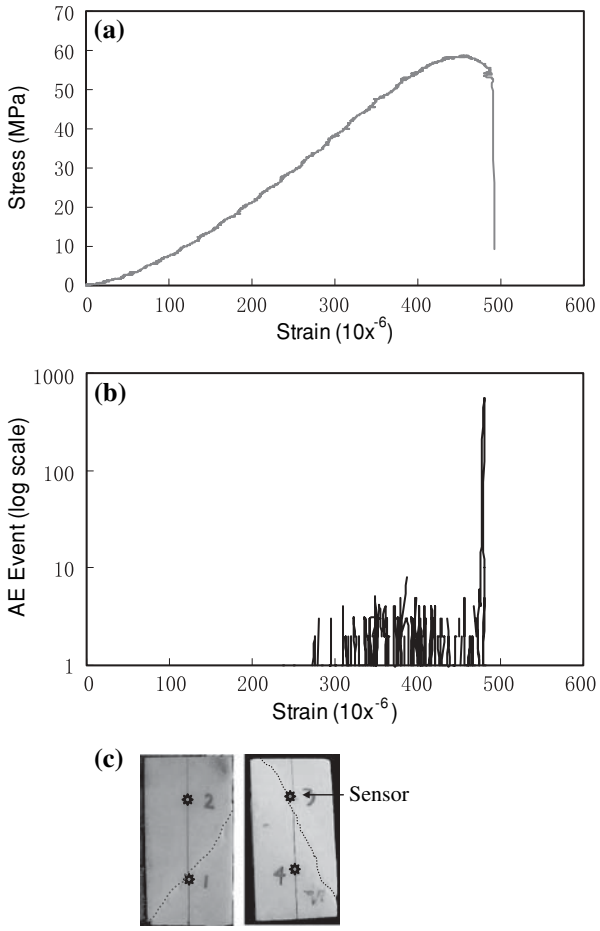

Figure 3
Experimental study on marble specimen with AE measurement. (a) Stress strain curve of marble under uniaxial compression, (b) AE events vs strain of specimen under compression, (c) failure mode of the specimen.

RFPA^{2D} is a progressive "elastic-damage model." Using elastic stress analysis, stress and deformation in each element of a sample is calculated for every loading step. When the stress in some elements within the specimen reaches a critical strength, these elements will fail either in shear or in tension. A Coulomb criterion with a tension cut-off is used as a failure criterion to determine whether each element fails in shear or in tension. When each element fails, an AE event is reported. To overcome the numerical instabilities, the failed elements are given with a small, but non-zero, elastic modulus. Thus, in reality the failed elements were neither removed from the mesh nor from the stress analysis. The elastic modulus of element reduces to $(1-D_e)E_o$ from E_o after failure, where $D_e = 1 - \sigma/(E_o\varepsilon)$ depending on the current

reduced stress level (normally taken as 1/10 of the peak strength) and strain at the element. The Poisson's ratio v for all the elements is assumed to be constant throughout the deformation. When an element fails, this element will not resist pressure because stress will redistribute around this damaged element instantaneously. Within some elements at other positions, where stress increases due to stress redistribution, the local stress may exceed the critical value and hence further failure will result. The iterative process of checking failure is repeated until no more failure at other elements occurs. Then, the next increment of loading can be applied and the same iterative procedure can be used to trace the failed elements in the next loading step. Once the global load-bearing capacity of the specimen drops, the strength can be obtained. In this model, owing to a constant Poisson's ratio that is assumed, no anisotropy failure occurs in a element level. But for global damage, this model has anisotropy failure. The friction angle is not changed after failure of a residual friction angle is assumed in the numerical model.

The two-dimensional FEM mesh for a specimen of 50 mm × 100 mm (width × height) is a 92 × 184 mesh (or 16,928 elements); that is, element size equal to the grain size of the Chinese marble. The calibrated input parameters for the numerical simulations are listed in Table 3. The value of σ_0 and m is the result of microcracks statistics obtained from Table 2. The value of E, υ and σ_c/σ_t is the experimental result obtained from Table 1. The specimen is assumed to undergo plane strain deformation. An external displacement is applied at a constant rate of 0.0005 mm/step in the axial direction.

Seismic Events

The RPFA^{2D} code can simulate the damage of initiation and propagation causing seismic energy release during the unstable failure of brittle rock (TANG and KAISER, 1998). It is assumed that the radiated energy is equal to the energy stored in the element before failure is triggered. Due to the heterogeneity of rock properties, seismic quiescence may occasionally occur with the nucleation zone. The cumulative seismic damage calculated based on the seismic event rate form the simulation can be used as a damage parameter to describe the damage evolution.

The energy e_f released by the failure of each element can be calculated by the peak strength of the failed element.

$$e_f = \frac{1}{2E_f}\sigma_{cf}^2.v_f \tag{6}$$

Table 3

Material parameters for numerical simulation

Element number	σ_0 (MPa)	m	E (GPa)	υ	σ_c/σ_t	ϕ (°)
(50/0.54 × 100/0.54) = 92 × 184 = 16,928	290	1.76	47.74	0.29	10	30

where E_f is the elastic modulus for the element, σ_{cf} is the peak strength of the failed element and v_f is the volume of the individual failed element. The cumulative seismic energy can then be obtained by

$$e = \sum e_f = \sum \frac{1}{2E_f}\sigma_{cf}^2 . v_f = \frac{v_f}{2}\sum \frac{\sigma_{cf}^2}{E_f}. \tag{7}$$

The magnitude, m_f of an individual microseismic event or the magnitude M_f of a seismic event cluster can then be obtained by the following equations:

$$m_f = \log(e_f) + C, \tag{8a}$$

and

$$M_f = \log\left(\sum_{i=1}^{n} e_{fi}\right) + C, \tag{8b}$$

where C is a constant and i is the number of events in an event cluster. By using the calculated results form Equations (6) to (8), a frequency-magnitude relation can be obtained for each step and for both microseismic events and seismic events of cluster.

The results of the numerical simulations and the comparison with the experiment is presented in the next section.

Discussions

Using the micromechanical parameters, numerical simulations have been conducted and the results are given in Figure 4. More specifically, stress-strain curve is given in Figure 4(a) and the AE events associated with elemental failures are plotted in Figure 4(b). To illustrate the process of progressive failure, both the failed elements and the associated AE events were shown in Figure 5. The simulated uniaxial compressive strength is 48.83 MPa which is about 16% lower than that of the experiment (58.51 MPa). Furthermore in Figure 4(a), it is observed that there is still residual stress of 10–15 MPa after peak stress, although such residual stress is not observed in the experiment which is under compression stress without confining pressure (Fig. 3(a)). The residual stress existing in the modelling specimen is due to the elements which are confined by the adjacent elements. This confinement can be treated as a kind of confining pressure to the elements within the specimen. Thus, residual strength may exist. In addition, it is observed that the stiffness increases at the beginning of the loading (Fig. 3(a)), while a softening regime appears before the brittle failure. However, these two features are not captured by the numerical model. Actually, the marble specimen contains pores and cracks. The increased stiffness at the beginning of the load may be due to the closing of the microcracks and pores. The stress-strain curve from plastic deformation changes to elastic deformation.

However for the modeling specimen, the heterogeneity of rock is generated by using the Weibull distribution. Strong elements and weaker elements are generated according to the *m* value (heterogeneity index). No real cracked element is generated in the modeling specimen. Thus, no cracks or pores close the process in the modeling specimen at the beginning of the applied loading. For the softening regime appearing before the brittle failure of the experiment, as it is known before the brittle failure some of the cracking may start jointing together. Thus, stress would not increase and the softening regime would appear. The size of the softening regime depends on the rate of crack growth and coalescence process. However, for the modeling specimen, the softening regime depends on the number of failure elements. It was observed that a small amount of elements fails before the brittle failure, and stress drops slightly. After two steps displacement, a large number of elements fail and form a rapid drop of stress-strain curve. The modeling result has a softening regime but appears only within three steps (Fig. 4(a)). Although there are discrepancies in the strength and

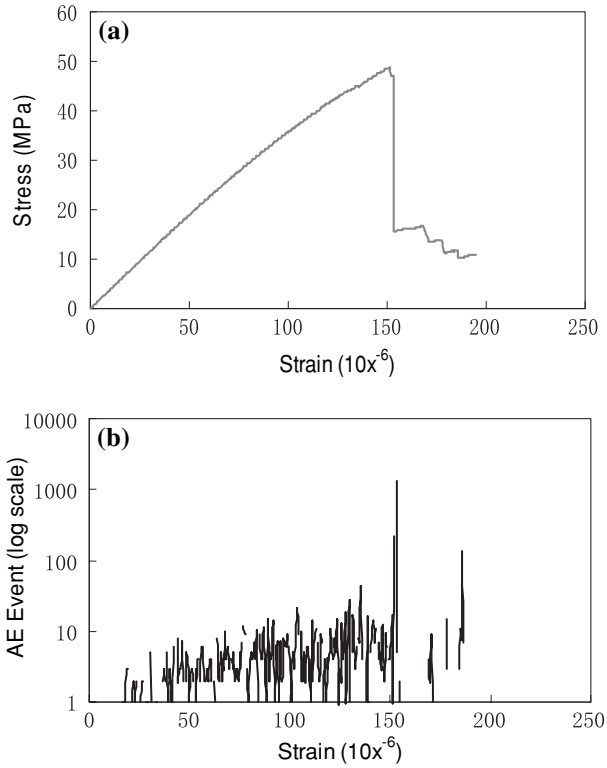

Figure 4
Numerical simulation using the micromechanical Weibull parameters. (a) Stress strain curve, (b) AE counts.

stress-strain curve, the general and failure patterns for both experiment and simulation are similar (compare Figs. 3(a) and 4(a)). In particular, the stress-strain curves drop rapidly after the peak for both experiment and simulation, and this characterizes the behavior of a brittle rock.

For AE pattern, both experiments (Fig. 3b) and numerical simulation (Fig. 4b) show a main-shock type seismic pattern. In the experiment of Fig. 3(b), the maximum AE event appears before the brittle failure. It is believed some of the AE signal data loss occurs during the failure process, because there are too many AE signals induced during the failure process. Thus, some of data are overlapped and cause the data loss. For the numerical model, the AE signal can be captured before and after the failure.

The failure process of the specimen is shown in Figure 5. The first row shows the stress distribution of the specimen and the second row shows the AE location under compression. The black color in the specimens of the first row represents the failed element. The white and red colors in the specimens of the second row represent the failure nature of each element under compression and tension, respectively. The radius of each circle is proportional to the stress drop of the element. It is noted that both tensile and compressive failure are induced under compressive loading. The ultimate failure is mainly in the tensile mode but with macroscopic shear coalescence. The failure pattern of numerical simulation agrees well with the experiment (Fig. 3(c)).

It is moreover to confirm that there are various ways to formulate a microcrack size distribution in relating to the Weibull parameters to simulate the progressive

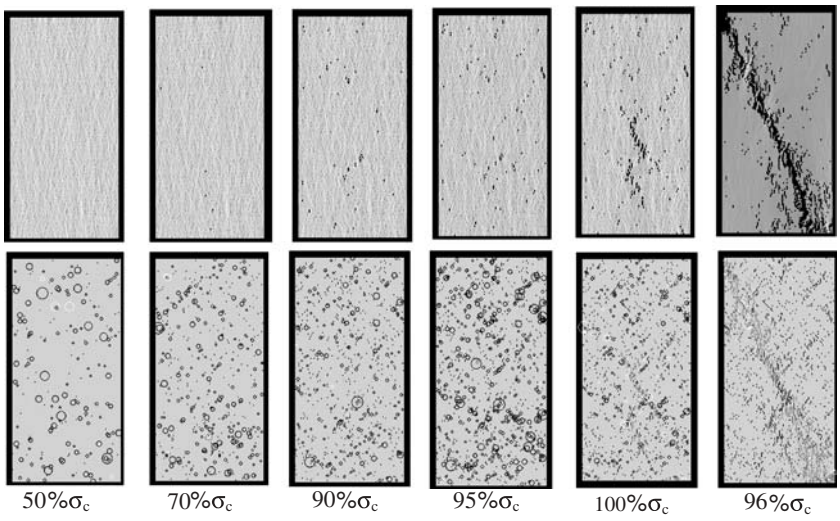

Figure 5
Failure process under compression (numerical simulation). The σ_c represents the peak strength. The first row shows stress distribution. The second row shows the AE location where the white and red color represents the failure element under compression and tension, respectively.

failures of heterogeneous rock specimens under compression. It is worthwhile for us to use the micromechanical parameters to apply to the other numerical models, which were developed to capture the progressive failure of rock. For example, the discrete element method (DEM, (CUNDALL and STRACK, 1979). This model can produce many features of rock such as fracturing, acoustic emission, damage accumulation, etc. (POTYONDY *et al*., 1996). The strength property determined by using the statistic of crack distribution can be used as microproperties of strength parameter for the particles.

Conclusions

This study presents a realistic numerical simulation using micromechanical parameters. The micromechanical parameters (or Weibull parameters) related to grain size and crack statistics are input into the RFPA^{2D} (Rock Failure Process Analysis code) to generate the heterogeneity of natural rocks and to study the failure process of rock. A compression test was conducted on a specimen of marble found in mainland China, and the acoustic emissions (AE) associated with cracking are recorded. Based on the numerical simulation and experimental studies, although there are discrepancies in the strength and stress-strain curve, the general and failure patterns for both experiment and simulation are similar in which a rapid drop of stress is observed after the peak stress. The AE pattern in both experiment and simulation are the main-shock type. The observed and predicted failure modes are similar. The failure process is mainly tensile but with macroscopic shear coalescence. This paper further confirms that the micromechanical parameters approach for numerical simulation is a more realistic method to simulate the failure process of rock.

The present paper proposes to plot the crack statistics using the crack count per scanned volume per grain size to yield the required Weibull parameters. It is found that the crack statistics will change with the scanned area and the length interval. Thus, it is of value to carry out a detailed examination to interpret the crack data. In addition, more carefully designed experiments will also be conducted on various kinds of rocks such as granite and sandstone with various grain sizes. It is of interest to explore the extent to which the influences on compressive failure behaviour are similar to the observations in this study. Furthermore, it is beneficial for us to use the micromechanical parameters to apply to the other numerical models which were developed to capture the progressive failure of rock.

Acknowledgments

The study was supported by Hong Kong Polytechnic University to RHC Wong (A-PD49 and A-PE31). We are grateful to Professor Teng-fong Wong, the Professor

of State University of New York at Stony Brook, for formulating the relations between microcracks and Weibull parameters and on how to interpret microcrack data, and to Prof. L. G. Tham of HKU for allowing us to use the facilities at their rock mechanics laboratory.

References

ARGON, A.S. (1974), *Statistical aspects of fracture*, Composite Mater. *5*, 153–189.

ASTM (1995a), *Standard test method for unconfined compressive strength of intact rock core specimens*. Test Designation D2938-95 Annual book of ASYM standards, American Society for Testing and Materials, Philadelphia (*14*) 02.

ASTM (1995b), *Standard test method for elastic moduli of undrained intact rock core specimens in biaxial compression*. Test Designation D3148-95 Annual book of ASYM standards, American Society for Testing and Materials, Philadelphia. (*14*) 02.

ASTM (1995c), *Standard test method for splitting tensile strength of intact rock core specimens*. Test Designation D3967-95a Annual book of ASYM standards, American Society for Testing and Materials, Philadelphia (*14*) 02.

ASTM (1995d), *Standard test method for triaxial compressive strength of undrained rock core specimens without pore pressure measurements*. Test Designation D2664-95 Annual book of ASYM standards, American Society for Testing and Materials, Philadelphia (*14*) 02.

ATKINSON, B.K. *Fracture Mechanics of Rock,* Academic Press Geology Series (Academic Press Inc., London Ltd., (1987)).

BROWN, E.T. (1981), *Rock Characterization Testing and Monitoring, ISRM Suggested Methods*: *Suggested Method for Petrographic Description of Rocks,* International Society for Rock Mechanic, pp. 73–77.

CUNDALL, P.A. and STRACK, O.D.L. (1979), *A discrete numerical model for granular assemblies,* Geotechnique *29*, 47–65.

DOBSON, D.P., PHILIP, G., MEREDITH, S., and BOON, A. (2004), *Detection and analysis of microseismicity in multi-anvil experiments,* Phys. Earth Planet. Interiors 143–144, 337–346.

FANG, Z. and HARRISON, J.P. (2002), *Development of a local degradation approach to the modeling of brittle fracture in heterogeneous rocks*, Int. J. Rock Mech. Min. Sci. *39*, 443–457.

FENG, X.T., CHEN, S.L., and ZHOU, H. (2004), *Real-time computerized tomography* (*CT*) experiments on sandstone damage evolution during triaxial compression with chemical corrosion, Int. J. Rock Mech. Min. Sci. *41*, 181–192.

HEIDELBACH, F., KUNZE, K., and WENK, H.R. (2000), *Texture analysis of a recrystallized quartzite using electron diffraction in the scanning electron microscope,* J. Struct. Geology *22*(1), 91–104.

HOMAND, F.D., HOXHA, T., BELEM, M., PONS, N., and HOTEIT, N. (2000), *Geometric analysis of damaged microcracking in granites*, Mech. Mater. *32*, 361–376.

ISRM (1988), *Suggested Method for determining fracture toughness of rock* (*F. Ouchterlony, Working Group Coordinator*). Int. J. of Rock Mech. Min. Sci. Geomech. Abstr. *25*, 71–96.

JIAO, M.R., WONG, R.H.C., WONG, T.F., CHAU, K.T., and TANG, C.A. (2004), *Numerical simulation of the influence of grain size on the progressive development of brittle failure in Yuen Long marbles*, Key Eng. Mater. 261–263, 1511–1516.

KAWAKATA, H., CHO, A., KIYAMA, T., YANAGIDANI, T., KUSUNOSE, K., and SHIMADA, M. (1999), *Three-dimensional observations of faulting process in Westerly granite under uniaxial and triaxial conditions by X-ray CT scan*, Tectonophysics *313*, 293–305.

LAWN, B. *Fracture of Brittle Solids*, Second Edition (Cambridge University Press, Cambridge, (1993)) 378 pp.

LIN, P., WONG, R.H.C., CHAU, K.T., and TANG, C.A. (2000), *Multi-crack coalescence in rock-like material under uniaxial and biaxial loading*, Key Engin. Mater. 183–187, 809–814.

LIU, H.Y., KOU, S.Q., LINDQVIST, P.A., and TANG, C.A. (2004), *Numerical studies on the failure process and associated microseismicity in rock under triaxial compression*, Tectonophysics *384*, 149–174.

MOGI, K. (1962), *Study of elastic shocks caused by the fracture of heterogeneous materials and their relation to earthquake phenomena,* Bull. Earthq. Res. Inst., University Tokyo *40*, 125–173.

MCCLINTOCK, F.A. and ARGON, A.S. *Mechanical Behavior of Materials*. Addison-Wesley, Reading, MA., (1966) 504–508. pp.

MOWAR, S.M., ZAMAN, D., STEARNS, W., and ROEGIERS, J.-C. (1996), *Micro-mechanisms of pore collapse in limestone*, J. Petroleum Sci. Eng. *15*, 221–235.

POTYONDY, D.O., CUNDALL, P.A., and LEE, C. (1996), *Modeling rock using bonded assemblies of circular particles*, Proc. North Am. Rock Mech. Symp. *2*, 1937–1944.

TANG, C.A. WANG, W.T., FU, Y.F., and XU, X.H. (1998), *A new approach to numerical method of modeling geological processes and rock engineering problems-continuum to discontinuum and linearity to nonlineartiy*, Eng. Geology *49*(3–4), 207–214.

TANG, C.A. and KAISER, P.K. (1998), *Numerical simulation of cumulative damage and seismic energy release during brittle rock failure - Part I: Fundamentals*, Int. J. Rock Mech. Min. Sci. *35*(2) 113–121.

TANG, C.A., LIN, P. WONG, R.H.C., and CHAU, K.T. (2001), *Analysis of crack coalescence in rock-like materials containing three flaws-Part II: Numerical approach*, Int. J. Rock Mech. Min. Sci. *38*, 925–939.

WEIBULL, W. (1951), *A statistical distribution function of wide applicability*, J. Appl. Mech., *18*, 293–297.

WONG, T-F., WONG, R.H.C., JIAO, M.R., CHAU, K.T., and TANG, C.A., (2004), *Micro-mechanics and rock failure process analysis*, Key Eng. Mater. 261–263, 39–44.

WONG, T-F., WONG, R.H.C., CHAU, K.T., and TANG, C.A. (2005), *Microcrack statistics, Weibull distribution and micromechanical modeling of compressive failure in rock*, J. Mech. Mater. *38*, 664–681.

WU, X.Y., BAUD, P., and WONG, T.F. (2000), *Micromechanics of compressive failure and spatial evolution of anisotropic damage in Darley Dale sandstone*, Int. J. Rock Mech. Min. Sci. *37*, 143–160.

YOUNG, R.P. and COLLINS, D. S. (2001), *Seismic studies of rock fracture at the Underground Research Laboratory*, *Canada*, Int. J. Rock Mech. Min. Sci. *38*(6), 787–799.

YUAN, S.C. and HARRISON, J.P. (2004), *Numerical modelling of progressive damage and associated fluid flow using a hydro-mechanical local degradation approach,* Int. J. Rock Mech. Min. Sci. *41*(3), paper 2A 01.

(Received December 28, 2004, revised July 8, 2005, accepted August 29, 2005)
Published Online First: September 2, 2006